Electronic Supplementary Material (ESI) for Journal of Materials Chemistry A.

Fabrication of Triboelectric nanogenerators with multiple strain mechanisms towards High-accuracy material and gesture recognition

Junjun Huang[a,c], Wenqing Zhang[a,b], Xin Chen[a], Sanlong Wang[a,b], Zhenming Chen[a,c], Peng Li[c], Honglin Li[a,b,c**] and Chengmei Gui[a,b,c*]

[a] *School of Energy Materials and Chemical Engineering, Hefei University, Hefei City, 230601 China*
[b] *School of Chemistry and Chemical Engineering, Chaohu University, Hefei City, 230009, China*
[c] *Guangxi Key Laboratory of Calcium Carbonate Resources Comprehensive Utilization, College of Materials and Chemical Engineering, Hezhou University, Hezhou City, 542899, China*

Corresponding Authors: *Chengmei Gui E-mail: huangjunjun163@163.com
** Honglin Li E-mail: lihonglin163163@163.com
*** Peng Li E-mail: lipeng163163163@163.com

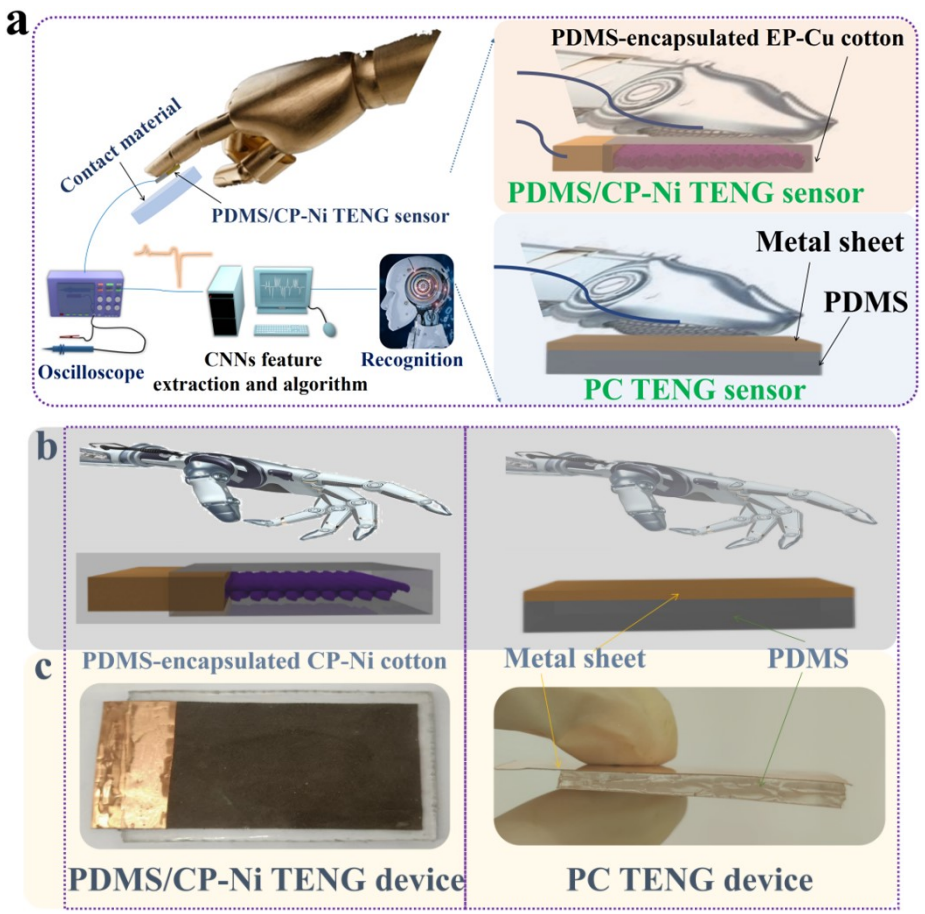

Fig. S1. Schematic diagram of the application of intelligent prosthesis (a). Structural diagram (b) and optical photograph (c) of PC and PDMS/CP-Ni TENG devices

The schematic diagram of the application with intelligent prosthesis are displayed in Fig. S1 a. Fig. S1 b and c displayed structural diagram of PC and PDMS/CP-Ni TENG devices. Similar to a closed sandwich structure, the CP-Ni cotton is located in the middle layer, one side leads out the electrode, the others are sealed in the PDMS layer (PDMS/CP-Ni TENG device). In this structure, the polymer surface acts as a negative electrode. To further verify the unique characteristics of PDMS/CP-Ni TENG device, we fabricated the conventional TENG device of single electrode mode: triboelectric material (PDMS layer) coated on the Cu sheet surface (PC device). the thickness of the two devices is 0.234 cm in this work. Corresponding optical photograph of PC and PDMS/CP-Ni TENG devices is displayed in Fig. S1 c.

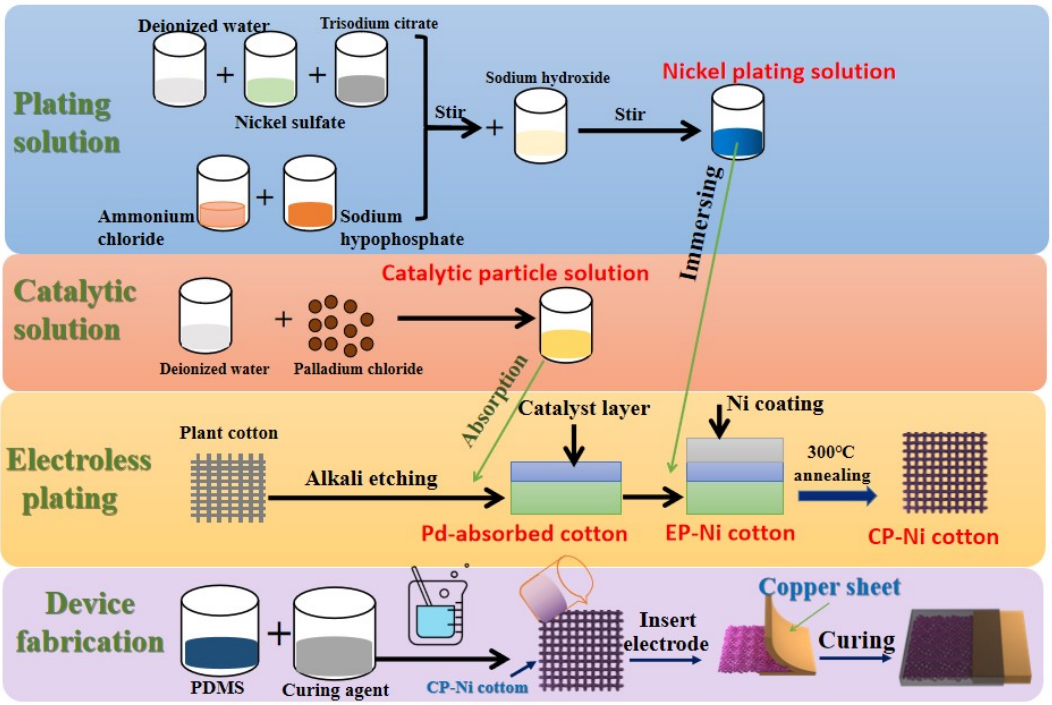

Fig. S2. Schematic diagram of the fabrication process of PDMS/CP-Ni TENG device

Fabrication of Catalytic layer: $PdCl_2$ (0.2 g/L, pH is 2) solution was fabricated and used as catalytic solution. The cotton sheet was cleaned by degreased solution, acetone beforehand and deionized water, in sequence at 333 K for 60 min, respectively. The cleaned substrate surface was immersed in catalytic solution for 30 min. Afterward, the sample was rinsed in a water bath for several minutes followed by drying with blown nitrogen. As a result, catalytic layer by means of Pd nanoparticles/polymer brush structure on sample surface was fabricated (AC-Ni cotton).

Electroless Plating: The AC-Ni cotton was plated using a reported solution. The components of the plating solution is Nickel sulfate 15 g/L; Trisodium citrate 8 g/L; Ammonium chloride 18 g/L; Sodium hypophosphate 15 g/L; Ingredients and deionized water were mixed, and then heated to 60°C. After the bath was allowed to

stabilize to the plating 60°C, the catalytic layer-coated cotton was placed in the bath for the desired time. After plating, the plated sample was rinsed in a water bath for several minutes followed by drying and heating with blown nitrogen. The pH was measured using a pH meter, and found to maintain a steady pH of between 11.5 and 12 during the entire plating run. The schematic diagram of EP-Ni cotton can be seen in Fig. 1a and S2.

Fabrication of PDMS/CP-Ni TENG device: The EP-Ni cotton was annealed at 300 ℃ for 60 min, after that CP-Ni cotton was obtained. The curing agent and PDMS prepolymer (weight ratio of 1:12.5) were mixed. Firstly, the processed PDMS was evenly coated on the glass plate. Afterward, the CP-Ni cotton was inserted into the PDMS layer until it was entirely soaked. We adopted the polymer-encapsulated metal material with higher interfacial contact area to fabricate the PDMS/CP-Ni TENG device. Similar to a closed sandwich structure, the CP-Ni cotton is located in the middle layer, as displayed in Fig. S2. One side leads out the electrode, the others are sealed in the PDMS layer (PDMS/CP-Ni TENG device). In this structure, the polymer surface acts as a negative electrode. After being cured then heated at 120 ^{o}C for 1.5 h. After that, PDMS/CP-Ni TENG device was prepared.

Material and Characterization: The cotton composed of 80% cotton and 20% polyester was bought from the Wanchang Weaving Co. Ltd (Jinzhou, China), the gram weight is 105 g/m^2. The other experiments' materials were purchased from Aladdin Chemical Reagent Company (China) and used without further purification. Surface morphology was observed by scanning electron microscopy (SEM, JEOL,

JSM-5600LV). Chemical structure was measured by X-ray diffraction (XRD, Rigaku D/max-2550V) and X-ray photoelectron spectroscopy (XPS, Shimazu, AXIS ULTRADLD). XPS spectra was calibrated by using the C1s peak (284.5 eV). Thermogravimetric analysis (TG) was performed using a TA Instruments TGA5500 on the Electrifi filament by heating the material with a ramp of 20 °C/min until 800 °C. A Nitrogen flow rate was set to 10 mL/min.

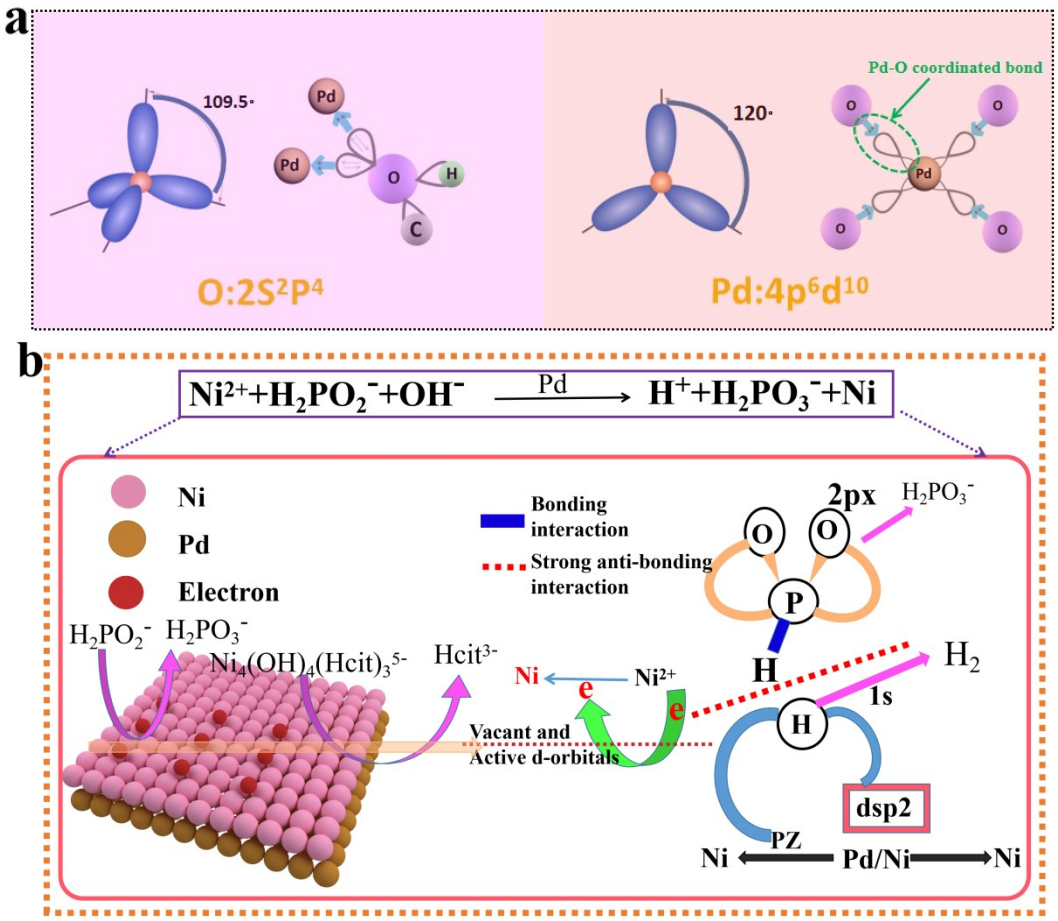

Fig. S3. Mechanism illustration of EP-Ni on cotton. Schematic illustration of the bonding formation between the O and Pd (a). Summarized structure of orbital interaction in $H_2PO_2^-$ on Pd/Ni surface (b).

Before the EP-Ni process, it is critical to establish catalytic sites (Pd particles) on the substrate surface. After dipping into activation solution ($PdCl_2$), the appearance of Pd signal in the XPS spectra, indicating that the Pd^{2+} is absorbed by active groups (Figure 1). To explicitly confirm the bonding mechanism, O 1s and Pd 3d XPS were used to characterize the electronic structure of these elements. Base on hybrid orbital

theory, Pd dsp2 orbital could be occupied by lone pair electrons from O ($2s^2$ $2p^4$) SP3 hybrid orbital, as displayed in Fig.S3 a. As a result, a strong force can be established between active groups (-COOH and -OH) and metal ion (Pd^{2+}), the force itself naturally takes on the form of coordinated bonds (Pd-O), indicating that both O adsorbed Pd through coordination effects (O-Pd) [1-4].

The absorbed Pd^{2+} can be reduced to Pd atom by reductant ($H_2PO_2^-$) in the plating solution. Tabulate the *REDOX* as follows:

$$Pd^{2+} + H_2PO_2^- + OH \longrightarrow H^+ + H_2PO_3^{2-} + Pd \quad (1)$$

In the EP process, Pd particles acted as catalyst to promote the reduction of Ni^{2+}. The deposited Ni atoms aggregated, connected and then nickel layers established. Based on general knowledge about the Pd electronic structure, it exhibits high catalytic activity for $H_2PO_2^-$ oxidation is because Pd has active d-orbitals and vacant. As displayed in Figure S3 b, in the occasion of $H_2PO_2^-$ adsorption on Pd surface, the P s-orbital interacts with the O p-orbital, whereas the H s-orbital interacts with d- and p-orbitals under Pd catalyst. These changes would facilitate the distortion of $H_2PO_2^-$ planar structure. The distortion effect derives from the coordination of electrons could be attributed to lone pairs in OH^- to the vacant p-orbital of P, which would cause new P-O bond to be constructed. This interaction decreased the $H_2PO_2^-$ stability. As a result, the efficient anti-bonding structure was established, follows by a strong P-H cleavage promotion effect. The less stable compound is converted into $H_2PO_3^-$ with dehydrogenation and charge transfer to Ni^{2+} through Pd d-orbitals and vacant [5,6], which result in the reduction of Ni^{2+} to Ni atoms. The reduced Ni can also be the medium, which cause Ni^{2+} continuously deposition. Overall, Ni coating was

established on PET surface (EP-Ni cotton).

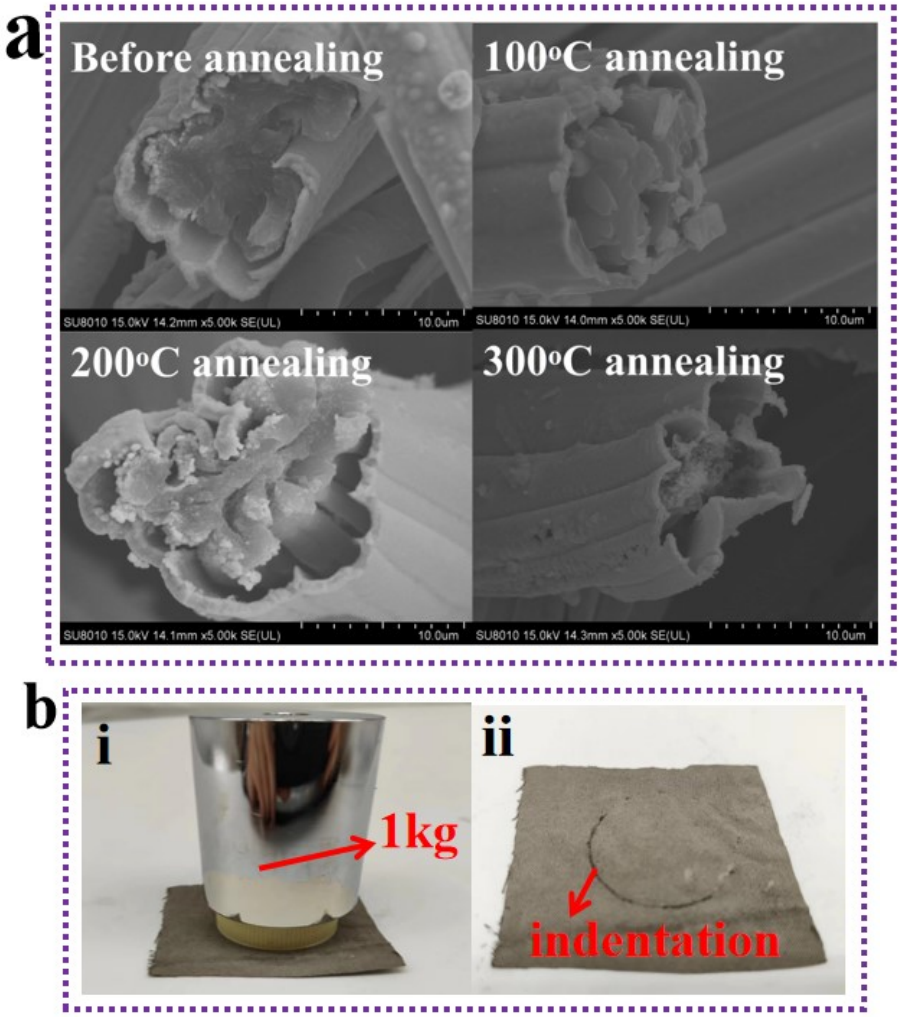

Fig. S4. Structural performance of 300℃ Ni electrode. (a) SEM images of annealed EP-Ni cotton at different temperature. (b) Compressive strength experiment result

Based on the above analysis, a micrometer double layer of grained Ni grain coated plant fiber yarn was prepared. Its two-layer structure is formed with plant fiber as the "core" and metal coating (nickel coating) as the "shell". Since the inner plant fiber is more sensitive to high temperatures than the nickel coating on the outer layer, the inside plant fiber can be carbonized into C tubes after annealing. From the SEM image in Fig.S4 a, we found that the plant fibers transform into amorphous carbon after annealing at 100-300 °C for 60 minutes. Thus, the 300 °C-annealed cotton is

consisted of amorphous carbon as a "core" and a nickel coating as a "shell". To be precise, textured Ni encapsulated C tube was fabricated successfully after annealing at 300 ^{o}C.

Here, under the same external force, the surface appearance of textile-based 300 ^{o}C-annealed cotton was analyzed to explore the role of compression characteristic, as displayed in Figures S4 b. We found indentation is established on CP-Ni cotton surface, indicating that the as-fabricated material belongs to brittle material, the Ni@C composite tube cracks under less stress.

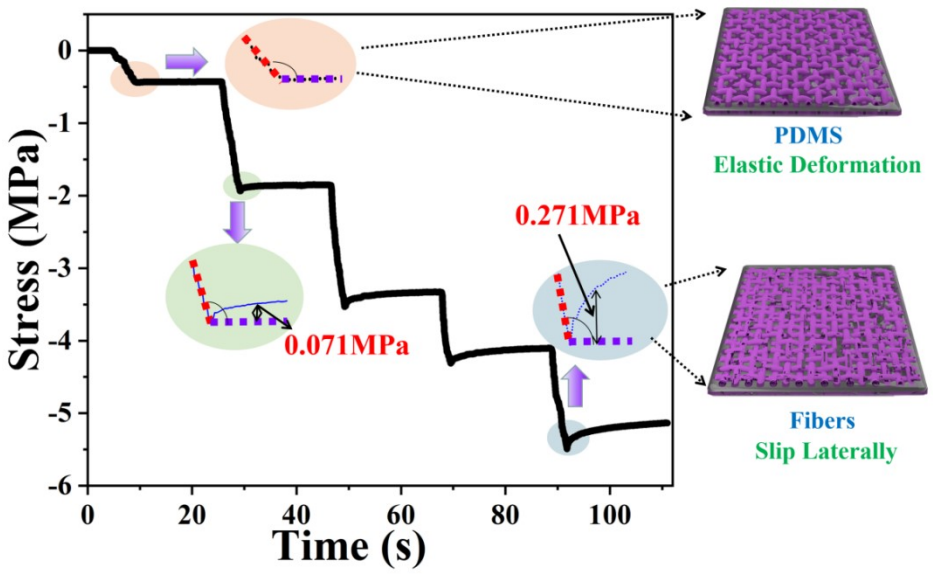

Fig. S5. The relationship between different stress and time on the surface of PDMS/CP-Ni TENG device

In order to study the deformation mechanism of samples under different compressive stresses. The different external stresses (0.44 MPa,1.90 MPa, 3.42 MPa, 4.24 MPa and 5.31 MPa) were applied to the PDMS/CP-Ni TENG device surface for about 19 s. The relationship between time and stress on the surface of PDMS/CP-Ni TENG device (true stress) was analyzed (Figure S5). To be precise, the creep behavior of sample under different stresses was analyzed. It

can be seen that, time has no effect on the true stress when external stress is 0.44 MPa (without creep behavior), indicating only PDMS compressive strain is established in the PDMS/CP-Ni material at lower external stress. Moreover, the true stress decreases gradually to 1.83 MPa with the increase of time, when external stress is enhanced to 1.9 MPa (creep behavior). Of note, the creep behavior becomes more and more obvious with the increase of external stress, indicating the fibers begin to slip laterally with the formation of larger material strain.

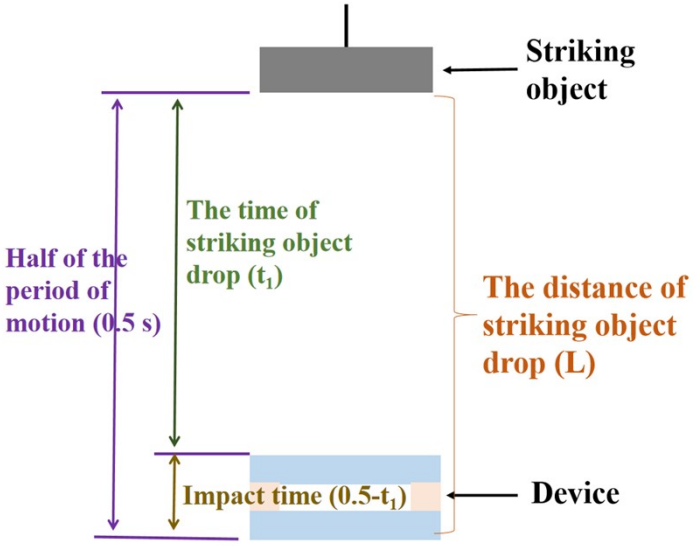

Fig. S6. Impact diagram of TENG device

The schematic diagram is described in Fig. S6 , the ε is adjusted by the weight and height of striking object in this work, the derivation of relationship between the two equals is as follows:

The time of striking object drop (t_1):

$$h = \frac{1}{2} g t_1^2 \Rightarrow t_1 = \sqrt{\frac{2h}{g}} \quad (2)$$

Where h is the height of a object's free fall. When it contacts with PDMS/CP-Ni surface, the rate of object (v):

$$v = gt_1 \quad (3)$$

Based on the law of momentum conservation and momentum balance:

$$F \times t_2 = m \times v = m\sqrt{2gL} \Rightarrow F = \frac{m\sqrt{2gL}}{0.5 - t_1} \quad (4)$$

Where t_2 is impact time between the two, which can measure it from the Figure S6. Thus, compressive stress on the PDMS/CP-Ni cotton can be calculated:

$$\varepsilon = \frac{F}{S} \quad (5)$$

Where the S represents compression area (radius is 1.95 cm). We can calculate the V_{oc}-ε relationship, which is displayed in the Fig. 2d.

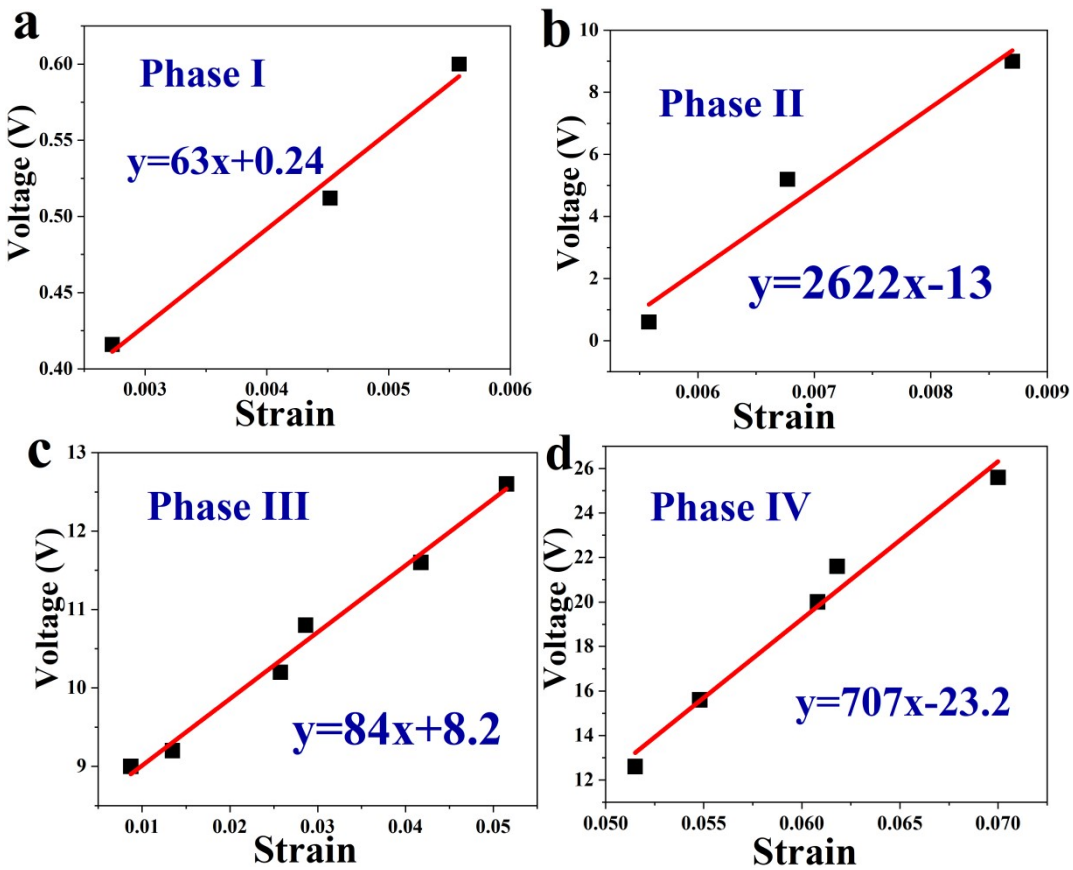

Fig. S7. Schematic diagram of output voltage test under different strain (a-d)

Fig. S7. a-d displayed schematic diagram of output performance test under different stresses. We found the curve is linear in the strain range of 0-0.0055, 0.056-

0.0088, 0.009-0.052 and 0.053-0.072, and its correlation can be fitted and evaluated as below four equations with the enhancement of strain:

$$y = 63x + 0.24 \quad (6)$$

$$y = 2622x - 13 \quad (7)$$

$$y = 84x + 8.2 \quad (8)$$

$$y = 707x - 23.2 \quad (9)$$

As described in the above analysis, the output voltage-strain relationship of the as-fabricated PDMS/CP-Ni TENG devices is presented linear relation at different strain range.

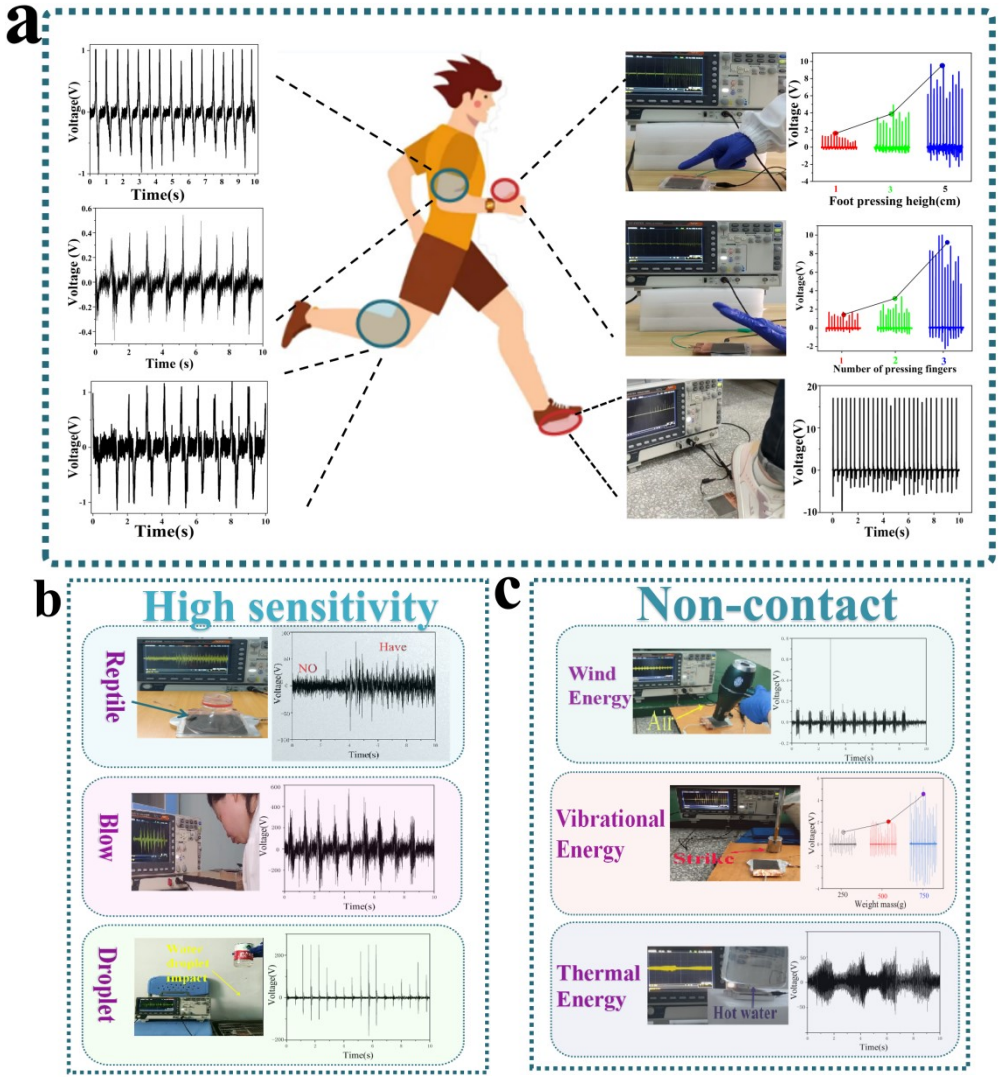

Fig. S8. The developed applications of as-fabricated TENG device. (a) Output voltage signal and testing photograph of PDMS/CP-Ni TENG device fixed to various parts of human body, (i)finger, (ii)palm, (iii) foot, (iv) underarm, (v) elbow and (vi) knee. (b) Output voltage signal and testing photograph of (i) reptile crawling, (ii) human blowing

and (iii) water droplets collision on the device surface. (c) Output voltage signal and testing photograph of (i) hair dryer blowing, (ii) knocking and (iii) hot water near the device surface.

From the results discussed so far, we can conclude that a fabric-based TENG device was successful fabricated. As proof of concept, we exhibit the possibility of the PDMS/CP-Ni TENG device as a bio-mechanical energy harvester to generate electricity from the motion of both large and subtle human movements in daily life. By utilizing the as-fabricated TENG device, we monitored a series of leg lifting, fingering, running, arm bending, and arm lifting as self-powered sensor, as displayed in Fig. S8 a. We can see that the maximum output V_{open} was ~10, ~10, ~20, ~1, ~0.6 and ~1 V, respectively, by fixing the fabric-based TENG to finger, palm, foot, underarm, elbow and knee (Fig. S8 a). It was owning to the compressive stress applied to the TENG device during human motion. In addition, various working mode and intensity endow our diverse with a variety of energy-harvesting method and sensitivity, As shown in Fig. S8 a, TENG is fixed to the finger, palm and foot, An increasing V_{open} can be find with the enhancement of number of pressing finger, the height of the palm clap and foot pressing height owning to higher stress/strain in the PDMS/CP-Ni device under the body percussive action, showing excellent sensing performance. To more vividly illustrate high sensitivity characteristics of devices, we investigate the output voltage of reptile crawling, human blowing and water droplets collision on the device surface, as displayed in Fig. S8 b, the V_{open} are ~100, ~600 and ~200 mV, respectively. Accordingly, we can believe the PDMS/CP-Ni TENG device can collect and transform some of the smaller mechanical energy. At present, all TENG device need to be in contact with external objects to convert energy, and non-contact sensors have not been reported. In order to expand the application

of TENG device, this work reveals several device working modes under non-contact conditions (wind, vibration and heat energy), the corresponding photographs and voltage waveforms are displayed in Fig. S8 c. It can be observed the PDMS/CP-Ni TENG device could transform wind, vibration and heat energy into electrical energy with ~0.2, ~7V and ~50 mV open-circuit voltage, of note, the device responded rapidly and generated stable output signals. From these results, the as-fabricated device demonstrated the ability to convert different energy such as vibration, raindrop, wind and human motions into electrical energy with excellent sensitivity.

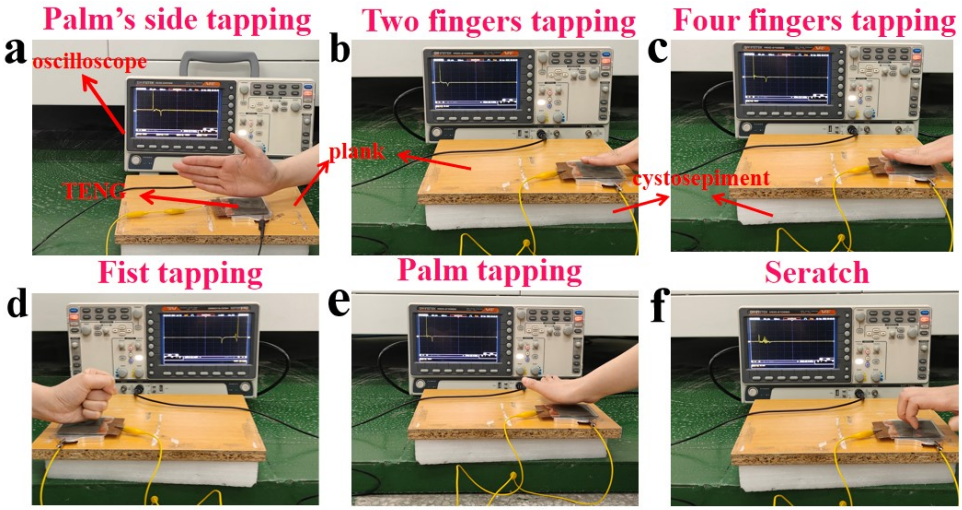

Fig. S9. Image of (a) palm's side tapping, (b) two fingers tapping, (c) four fingers tapping, (d) fist tapping, (e) palm tapping and (f) seratch

The schematic diagram of recognized object is described in Fig. S9 a-f, the PDMS/CP-Ni T-TENG device (4×8 cm) can be attached to test bench surface. In order to eliminate the effect of touch vibration on the background noise of output signal, a cystosepiment mat should be placed under the test table to reduce vibration (as depicted in Fig. S9 a-f). The volunteer hand with different gestures pressured the device surface. Acted on volunteer hand is unquantifiable, trying to ensure that the pressure stress is consistent, so that it obtains more meaningful practical applications. The output signal of the device is collected by oscilloscope.

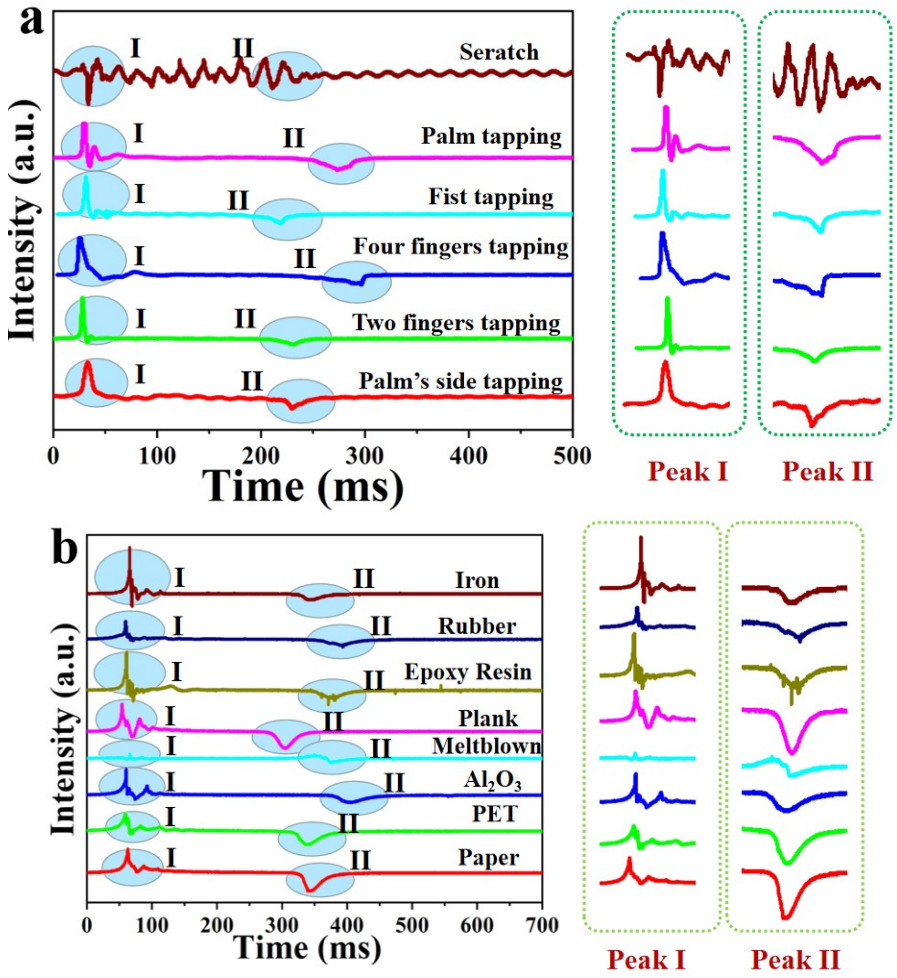

Fig. S10. The sensing signals from the as-fabricated TENG device as it recognizes different gestures (a) and materials (b)

The characteristics (peak position, spacing and shape) of signal curve from the TENG-based tactile sensor as the TENG impact the material and hand surface are used to recognize the unknown and contact object. The signals are presented in Fig. S10, obviously, the shape, number of characteristic peaks and distance between two peaks are different, i.e., the relative intensities of contact/separation peaks were inconsistent, the distance between the two peaks on the curve is also different.

More importantly, the signal from the PDMS/CP-Ni TENG device as it contacts different materials is a combination of output signals from PDMS/CP-Ni (Peak I in Fig. S10) and PDMS/recognize object (Peak II in Fig. S10) device. To be exact, there

are two TENG devices (PDMS/CP-Ni and PDMS/recognize object) that work when the as-fabricate PDMS/CP-Ni TENG devices under external stress.

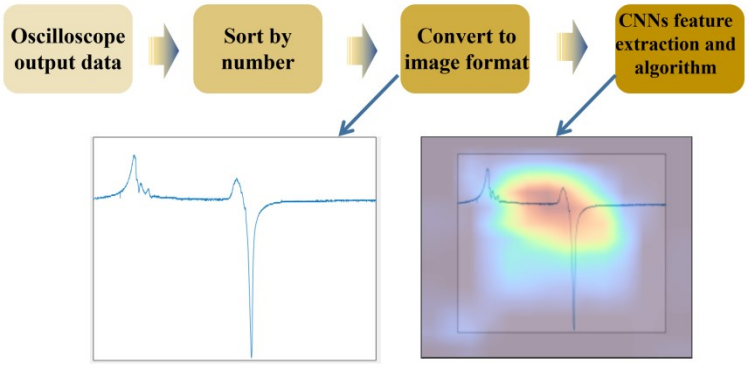

Fig. S11. Workflow of as-fabricate TENG touch sensing

Figure S11 displayed workflow of as-fabricated TENG touch sensing. The data from oscilloscope is numbered, formatted, CNNs feature extracted and recognized sequentially, then we can get the recognition result.

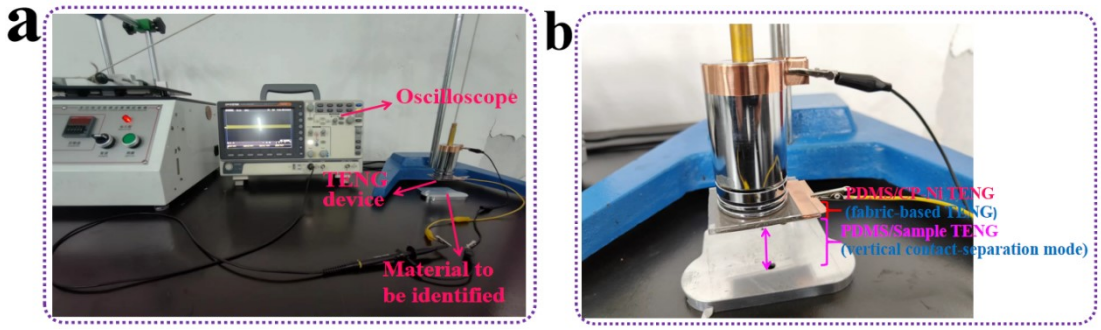

Fig. S12. Images of experimental setup using the TENG to accurate recognition

Output voltage signals are often influenced by contact material, contact pressure, and contact environmental conditions. In this work, the height of the object in free fall remained the same (10 cm), the mass of weights are 0.75 kg, respectively. The calculated compressive stresses on the devices is 79.5 KPa. The fixed positions of the device and target material are shown in the Figure S12 a. To be precise, two TENG devices, PDMS/CP-Ni (PDMS/CP-Ni TENG) and PDMS/sample (Figure S12 b), were established, resulting in the formation of two sensing signals from the PDMS/CP-Ni TENG sensor as it contacts different materials. We concluded

that various materials will provide different electrical signals, accompanied by unique characteristics, hence, the triboelectric signals generated by the as-fabricated TENG are capable of sensitive detection for contact materials. Extracting characteristics from multiple electrical signals offers exciting opportunities to achieve improving recognition accuracy. With the help of machine learning, more deep-rooted features of the identified materials are captured, and eventually achieve accurate identification independent of the environment.

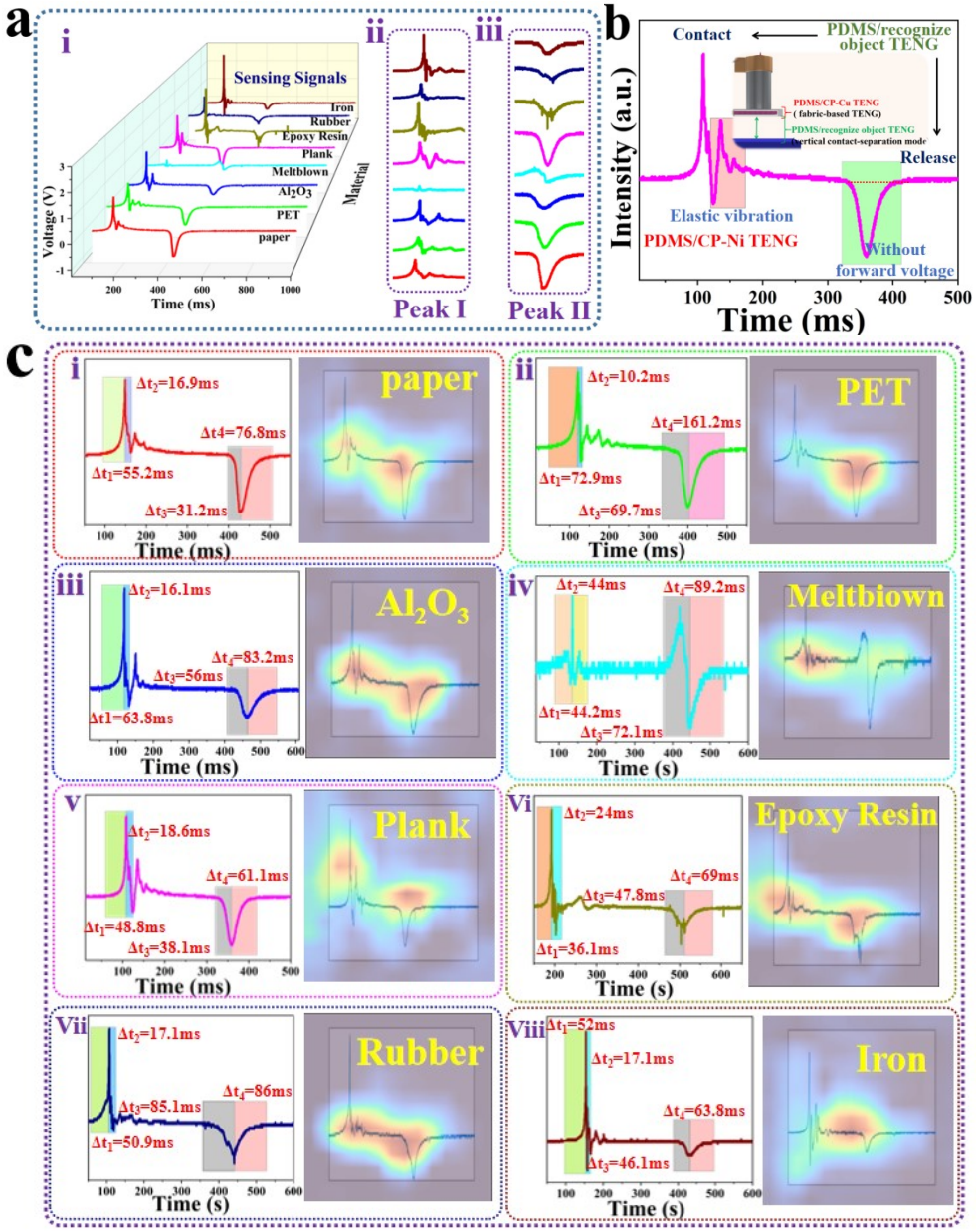

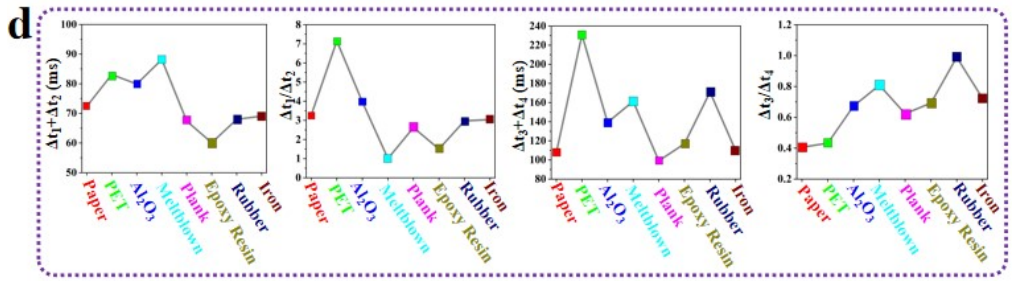

Figure. S13 The electric characteristics and sensing mechanism of the sensor. (a) 3D plots of output voltage signals responding to different materials. Corresponding (b,c) signal and (d) response time analysis.

The signals are presented in Fig. S13 a i-iii, obviously, the shape, number of characteristic peaks and distance between two peaks are different, i.e., the relative intensities of contact/separation peaks were inconsistent, the distance between the two peaks on the curve is also different, the wave-forms are also different. To explore the characteristics of the signals from the tactile sensor, peak I and II characteristics in typical signal curve are analyzed (Fig. S13 b). When the PDMS/CP-Ni TENG device touches an unknown material, the interface forces are transferred to the CP-Ni/PDMS layer interface through the PDMS layer, which would facilitate the introduction of friction between the CP-Ni/PDMS layer interface, causing the PDMS layer attenuating elastic vibration. The CP-Ni/PDMS layer contact-separation process is equivalent to a complete charge transfer process in a vertical contact-separation mode. Because the PDMS is wrapped around the CP-Ni material, the signal from CP-Ni/PDMS device is not two independent peaks, but a series of peaks of oscillation attenuation. This inter-facial force is affected by the surface structure of the unknown material, accompanied by unique characteristics (Fig. S13 a-c). It is important to highlight that the reported TENG tactile sensor do not output such characteristic signals.

Additionally, when the device is separated from the material, negative charges are accumulated on the PDMS, resulting in a negative voltage signal (peak II in Fig. S13). Except the signal curve of melt-blown, the peak II exhibited only a peak with an upward opening. The formation of two opposite characteristic peaks in meltblown curve is due to the lower elastic modulus. Given that the phenomenon of comprehensive dependence, one can conclude that there are two TENG devices (PDMS/CP-Ni and PDMS/recognize object) that works when the as-fabricated PDMS/CP-Ni TENG devices under 2.47-139 KPa stress. The signals from PDMS/recognize object TENG device is attributed to the difference in electron affinity and polarity between the PDMS and recognize object, however, PDMS/CP-Ni TENG device is owing to recognize object characteristics, i.e., surface roughness, structure, elasticity modulus. To be precise, the signal from the PDMS/CP-Ni TENG device is a combination of output signals from PDMS/CP-Ni and PDMS/recognize object device as it contacts different materials, the generated two signals (peak I and II in the Fig. S13 ii, iii and S9 b,c) are involved in CNNs feature extraction for following recognition. More importantly, the device demonstrates a low response time (the time to the first contact-peak/valley ($\triangle$t1) and to the first contact-valley/peak ($\triangle$t2), the second peak: $\triangle$t3 and $\triangle$t4, as marked in Fig. S13c i-viii). $\triangle$t1 and $\triangle$t2 values are range from 7.9 to 87.3 ms, manifesting the TENG signal is capable of higher sensitive detection for target object. Another interesting finding is that $\triangle$t1+$\triangle$t2, $\triangle$t1/$\triangle$t2, $\triangle$t3+$\triangle$t4 and $\triangle$t3/$\triangle$t4 value of the 8 different kinds of material present significant difference (Fig. S13 d), indicating triboelectric signals generated

by PDMS/CP-Ni TENG are distinguished. It is important to highlight that, as shown in the heat map for CNNs feature extraction from Fig. S13c i-viii, the red spot or 'hotspot" indicates the area where CNNs extracts the most characteristic information. As displayed in Fig. S13c i-viii, the red area appears around the both of peak I and peak II. Accompanied by unique characteristics, the TENG signals generated by the PDMS/CP-Ni and PDMS/recognize object device are capable of sensitive detection for contact materials.

REFERENCES

[1] J.D. Muller, K. Lamnawar, A. Maazouz, Relationship between rheological and surface properties for the sintering process of polymers, J. Mater. Sci. 47 (2012) 121-131. https://doi.org/10.1007/s10853-011-5773-4.

[2] D.X. Chen, Y. Zhang, T. Bessho, J. Sang, H.S. Hirahara, K, Mori, Z.X. Kang, Layer by layer electroless deposition: an efficient route for preparing adhesion-enhanced metallic coatings on plastic surfaces, Chem. Eng. J. 303 (2016) 100-108, https://doi.org/10.1016/j. cej.2016.05.114.

[3] C. Battocchio, C. Meneghini, I. Fratoddi, I. Venditti, M.V. Russo, G. Aquilanti, C. Maurizio, F. Bondino, R. Matassa, M. Rossi, S. Mobilio, G. Polzonetti, Silver nanoparticles stabilized with thiols: a close look at the local chemistry and chemical structure, J. Phys. Chem. C 116 (2012) 19571-19578, https://doi.org/10.1021/jp305748a.

[4] A.M. Venezia, X-ray photoelectron spectroscopy (XPS) for catalysts characterization, Catal. Today 77 (2003) 359-370, https://doi.org/10.1016/ s0920-5861(02)00380-2.

[5] M. Kunimoto, T. Shimada, S. Odagiri, Density functional theory analysis of reaction mechanism of hypophosphite ions on metal surfaces, J. Electrochem. Soc. 158 (2011) 585-589. https://doi.org/10.1149/1.3609000.

[6] M. Kunimoto, H. Nakai, T. Homma, Density functional theory analysis for orbital interaction between hypophosphite ions and metal surfaces, J. Electrochem. Soc. 158 (2011) 626-633. https://doi.org/10.1149/1.3623782.